Proceedings World Geothermal Congress 2020+1
Reykjavik, Iceland, April - October 2021

Lifetime and Energy Prediction of Geothermal Systems: Uncertainty Analysis in Highly Heterogeneous Geothermal Reservoirs (Netherlands)

Sanaz Saeid[a], Yang Wang[a], Alexandros Daniilidis[a], Mark Khait[a], Denis Voskov[a,b], David Bruhn[a,c]

[a]Delft University of Technology, Stevinweg 1, 2628 CN Delft, Netherlands. [b]Stanford University, CA 94305-4007, USA.

[c]Helmholtz Center Potsdam GFZ, Germany.

s.saeid@tudelft.nl

Keywords: geothermal energy, reservoir simulation, uncertainty analysis, low enthalpy

ABSTRACT

A good static and dynamic reservoir characterization is key for an accurate prediction of the lifetime and energy of geothermal systems. However, a deterministic reservoir model is not achievable mostly due to the lack of subsurface data and information. This can cause inefficient reservoir design and management, and might lead to decreased economic output.

An extensive uncertainty analysis of the physical and operational parameters can be invaluable in enhancing our understanding of a reservoir, hence increasing the prediction accuracy of its energy and lifetime. Nevertheless, uncertainty quantification by means of large simulation ensembles on a highly heterogeneous reservoir is always challenging and computationally very expensive.

In this work, the Delft Advanced Research Terra Simulator (DARTS) is used which can deliver fast and accurate production forecast of geothermal reservoirs. DARTS provides high computational performance due to the Operator Based Linearization (OBL) approach. This makes it an efficient tool for running an ensemble of simulations on complex geological models for uncertainty quantification.

In this study, we assess the effect of uncertainty in facies (consequently, in porosity and permeability) of a heavily channelized heterogeneous reservoir on the lifetime and produced energy of a geothermal system. A low-enthalpy geothermal field in the Netherlands has been chosen as the case study. The field consists of two main reservoir layers: one contains a heterogeneous sandstone; the other contains highly heterogeneous and channelized sand bodies. The study demonstrates that lack of data increases the uncertainty of lifetime and produced energy predictions of a geothermal system.

1. INTRODUCTION

In recent years, increasing the demand for energy while reducing environmental impacts of the energy sector have turned to major worldwide challenges (Fernández et al., 2017). The demand of energy not only grows in terms of electricity but also in the form of heat. In the Netherlands, more than 25% of the produced energy is consumed for heating purposes (CBS, 2018). The use of renewable energy, such as geothermal energy, in residential and industrial environments will help to meet the growing demands.

In the Netherlands, geothermal energy keeps growing in recent years. Heat production from low-enthalpy geothermal projects in the Netherlands has reached 3PJ in 2017. The produced energy is mainly used to heat commercial greenhouses and will be extended to enhance the heat network further. One of the promising geothermal regions is located in the West Netherlands Basin (WNB) (Donselaar et al., 2015). It accounts for 70% of all deep geothermal doublets currently in operation in the Netherlands. In addition, a research geothermal project targeting this formation will be employed on the TU Delft campus in the upcoming years ("Geothermal well," n.d.).

Uncertainty of data is one of the major difficulties in subsurface reservoir analysis including geothermal reservoir analysis. Direct wellbore core samples and logs usually are spared due to high costs. Therefore, subsurface models normally suffer from limited information, hence include uncertainties (Watanabe et al., 2010). To have a reliable geothermal reservoir model, a certain set of physical characteristics is required, the likelihood of fulfilling these requirements defines the risk in models. Therefore, the entire geothermal system needs to be characterized as precisely as possible. However, this is not the case in most of the situations due to lack of available data. Hence, uncertainty analysis plays a big role to quantify the risks involved in different stages of any geothermal systems project including exploration, development, and operation. In many cases, the source of uncertainty is rooted in the lack of geological data such as facies, porosity, and permeability distributions.

The prediction uncertainty of the numerical simulation and the risk estimate depend on the uncertainties associated with different reservoir parameters (Vogt et al., 2010). Saeid et al. (2015) have studied the effect of physical and operational parameters of a geothermal system on its lifetime and power production. They showed via a sensitivity analysis how the variation of geological (physical) parameters of a geothermal reservoir can affect its lifetime and produced energy. Willems and Nick (2019), show that the doublet lifecycle and heat recovery rate often vary a lot with both formation statistics and production management. Other studies have shown that similar results in terms of geothermal power can be achieved with different combinations of operational parameters (Daniilidis et al., 2016).

This paper addresses the uncertainty of reservoir geological parameters (facies, porosity, and permeability) and the prediction of geothermal reservoir lifetime in a field in the south-west of the Netherlands. Multiple realisations of reservoirs parameters have been generated and simulated. For the static modelling, the overall workflow comprises of a conditioning of the realization ensemble to up-scaled logs from the surrounding wells. The reservoir state variables are predicted from simulations of fluid flow and heat transport

for each realization. The statistic modelling for all realisations are made in Petrel, and Dynamic modelling are conducted in Delft Advanced Research Terra Simulator (DARTS, 2019).

Making 100s of uncertainty simulations is normally very computationally expensive due to the complexity of the physics and a large number of grid blocks in high-resolution geothermal models. DARTS includes high-performance capabilities for solution of forward and inverse problems for subsurface fluid and heat transport. For the solution of highly nonlinear problems, the Operator-based Linearization (OBL) approach is employed in DARTS, where besides conventional discretization in temporal and spatial space, discretization in the physical space is utilized (Voskov, 2017).

In the OBL approach, the mass and energy conservation equations are written in the summative form, where each term is split into the product of two operators depending on the physical state and the spatial properties respectively. The operators depending on the physical state are represented in an approximate form using physical supporting points and multilinear interpolation between them. This representation simplifies the linearization process since the complex physics is translated into a generic interpolation calculated in an adaptive way (Khait and Voskov, 2018b). As a result, the programming code is significantly simplified with enough flexibility and high performance in favor of the OBL approach. Furthermore, the architecture of the code supports shared memory parallelism and farther extension to GPU programming (Khait and Voskov, 2017).

2. GOVERNING EQUATIONS AND OBL APPROACH

Here, we consider the governing equations and nonlinear formulation for two-phase thermal simulation with aqueous brine. This problem can be described by mass and energy equations:

$$\frac{\partial}{\partial t}(\phi\rho_w) - div\,(K\frac{\rho_w}{\mu_w}(\nabla p \quad - \gamma_w \nabla D)) + \rho_w \tilde{q_w} \sum_{j=1}^{n_p} \rho_j \tilde{q_j} = 0, \tag{1}$$

$$\frac{\partial}{\partial t}(\phi\rho_w U_w + (1-\phi)U_r) - div\,(Kh_w\frac{\rho_w}{\mu_w}(\nabla p \quad - \gamma_w \nabla D)) + div(\kappa \nabla T) + \rho_w \tilde{q_w} h_w = 0, \tag{2}$$

where: ϕ is porosity, ρ_w is the water molar density, U_w is the water internal energy, U_r is the rock internal energy, h_w is the water enthalpy, κ is the thermal conductivity, K is the permeability tensor, μ_w is the water viscosity, p is pressure, γ_w is the water gravity vector, D is depth.

2.1 Operator-Based Linearization (OBL)

Based on OBL approach (Voskov, 2017; Khait and Voskov 2018), all variables in the Eqs. (1) and (2), excluding ones from the phase source term, are expressed as functions of a physical state ω and/or a spatial coordinate ξ. Several simplifications and assumptions are applied here. In order to extend modelling to systems with precipitation and dissolution of chemical species, porosity is considered as a pseudo-physical state variable. This also reduces the number of state-dependent operators. Second, the rock internal energy and thermal conductivity are assumed to be spatially homogeneous.

Pressure and enthalpy are taken as the unified state variables of a given control volume following Faust and Mercer (1975) and Wong et al. (2015). Flux-related fluid properties are defined by the physical state of upstream block, determined at interface l. The state-dependent operator is defined as a function of the physical state only. The discretized mass conservation equation in operator form reads

$$\phi_0 V\big(\alpha(\omega) - \alpha(\omega_n)\big) + \sum_l \Delta t \Gamma^l (p^b - p^a)\beta(\omega) + \theta(\xi, \omega, u) = 0; \tag{3}$$

where,

$$\alpha(\omega) = (1 + c_r(p - p_{\text{ref}})) \sum_{j=1}^{n_p} \rho_j s_j\,; \qquad \beta(\omega) = \sum_{j=1}^{n_p} \rho_j^l \frac{k_{rj}^l}{\mu_j^l}. \tag{4}$$

The discretized energy conservation equation in operator form is as follows:

$$\begin{aligned} \phi_0 V\left(\alpha_{ef}(\omega) - \alpha_{ef}(\omega_n)\right) + (1-\phi_0)\mathrm{V}U_r\big(\alpha_{er}(\omega) - \alpha_{er}(\omega_n)\big) + \sum_l \Delta t \Gamma^l (p^b - p^a)\beta_e(\omega) \\ + \Delta t \Gamma^l (T^b - T^a) \sum_l (\phi_0(\varepsilon_{ef}(\omega) - \varepsilon_{ef}(\omega_n)) + (1-\phi_0)\kappa_r(\varepsilon_{er}(\omega) - \varepsilon_{er}(\omega_n))) \\ + \theta_e(\xi, \omega, u) = 0; \end{aligned} \tag{5}$$

where,

$$\alpha_{ef}(\omega) = \big(1 + c_r(p - p_{\text{ref}})\big) \sum_{j=1}^{n_p} \rho_j s_j U_j\,; \quad \alpha_{er}(\omega) = \frac{1}{\big(1 + c_r(p - p_{\text{ref}})\big)}; \quad \beta_e(\omega) = \sum_{j=1}^{n_p} h_j^l \rho_j^l \frac{k_{rj}^l}{\mu_j^l}; \tag{6}$$

$$\varepsilon_{ef}(\omega) = (1 + c_r(p - p_{\text{ref}})) \sum_{j=1}^{n_p} s_j \kappa_j\,; \qquad \varepsilon_{er}(\omega) = \frac{1}{(1 + c_r(p - p_{\text{ref}}))}. \tag{7}$$

This representation makes any complicated nonlinear physics significantly simplified. Instead of performing complex evaluations of properties and their derivatives with respect to nonlinear unknowns for every grid block at every iteration during the simulation, we can parameterize operators in physical space at the pre-processing stage or adaptively with a limited number of supporting points. The evaluation of operators during the simulation is based on multilinear interpolation which improves the performance of the linearization stage. In addition, due to the piece-wise representation of operators, the nonlinearity of the system is reduced which improves the nonlinear behavior (Khait and Voskov, 2018 a,b).

3. RESERVOIR GEOLOGY

The study area is located in the West Netherlands Basin which is an inverted rift basin. Sediments in this basin range in age from Jurassic to recent and are overlying Triassic and older sediments. The Upper Jurassic and Lower Cretaceous start with the continental sediments of the Nieuwerkerk Formation and Vlieland sandstone Formation [PanTerra, 2018]. These sediments were deposited in subsiding half-grabens, while adjacent highs were subjected to erosion. In these formations two main reservoir layers have been observed; these are the Berkel Sandstone, and the Delft Sandstone.

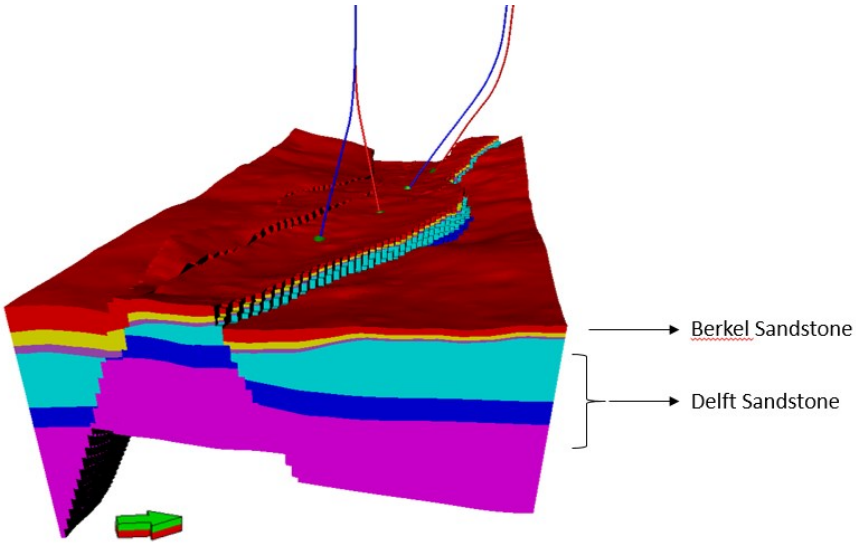

Figure 1: Structural model of the reservoir with identified layers.

The Berkel Sandstone Member and Berkel Sands-Claystone Member have a shallow marine depositional setting. The facies range from upper shoreface to lower shoreface of a coastal-barrier system. Lateral continuity is often good and cementation is low. The permeability of the sands is good to excellent ranging from 400 to >1000 mD. Porosities range from 20 to 30% (Figure 2).

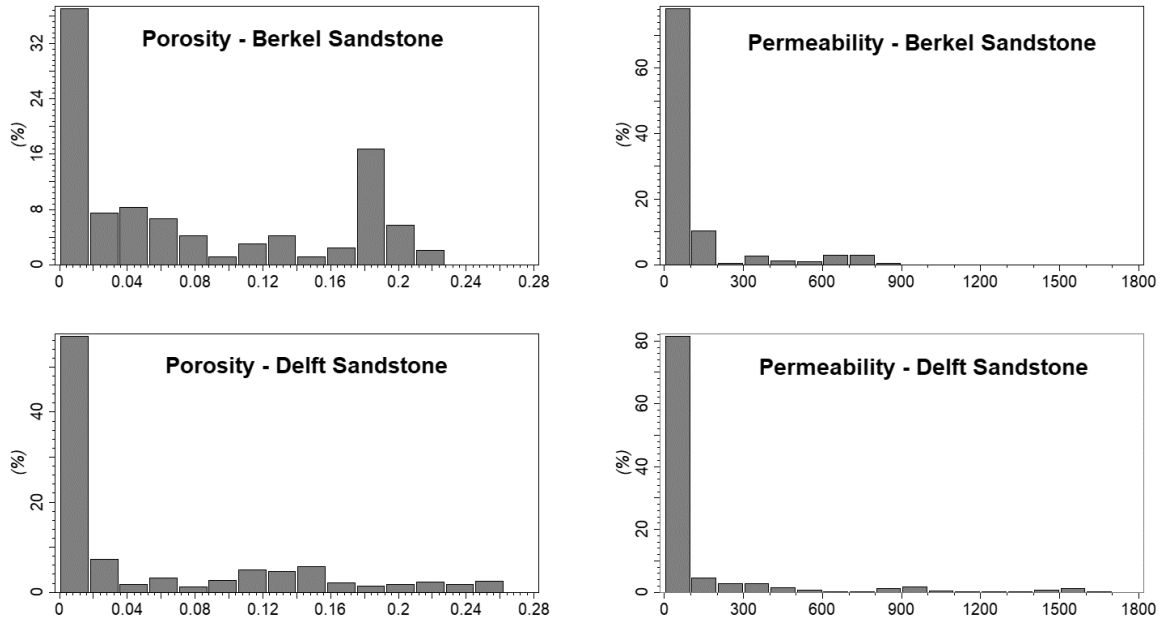

Figure 2: Histograms of porosity and permeability in Berkel and Delft Sandstones.

The Delft Sandstone is interpreted to be deposited as stacked distributary-channel deposits in a lower coastal plain setting resulting in massive sandstone sequences. The thickness of the Delft Sandstone is influenced by the syn-rift deposition of the sediments and therefore the Delft Sandstone is of variable thickness; a thickness up to 130m is observed [PanTerra, 2018]. The sandstone consists of fine- to coarse-grained sand, while the lateral continuity is difficult to predict. Porosities range from 10 to 27% and permeabilities from <100 to 2000 mD (Figure 2).

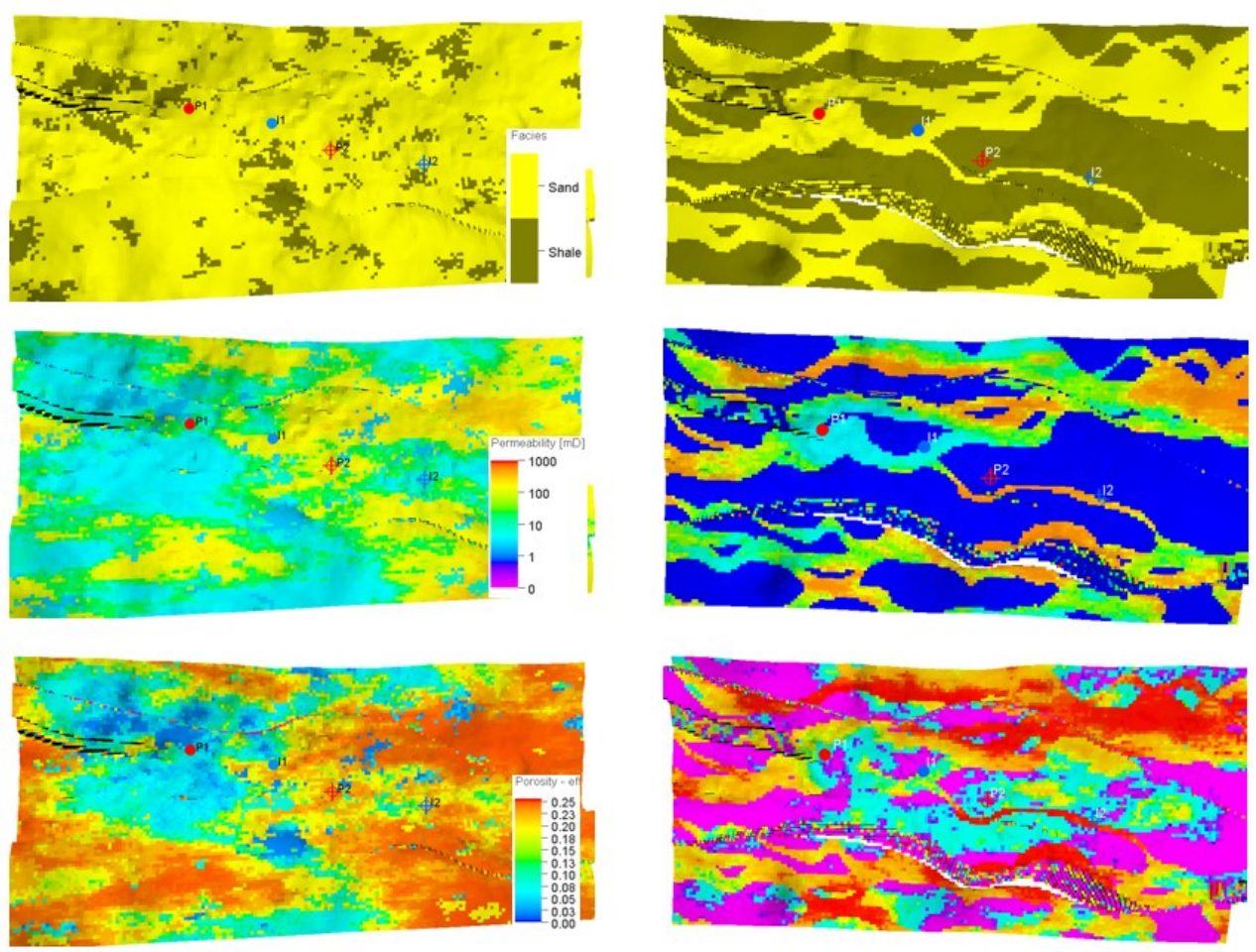

Figure 3: Base case properties. Left column: shows top of the Berkel Sandstone, and right column: shows top of Delft Sandstone. First row represents facies, second row shows Porosity, and third row shows Permeability.

Figure 3 shows the facies, porosity and permeability of both Berkel and Delft Sandstones based on the static model provided by the asset owner. The Delft Sandstone consist of irregular highly heterogeneous channels. In case of lack of data it is very difficult to predict the shape and location of the channels. This creates risk and uncertainty in designing the development of a geothermal system (e.g. well locations). In such cases, an uncertainty analysis is helpful to provide an understanding about possible shapes and locations of the channels, and to assist towards a better well positioning design.

4. GEOTHERMAL RESERVOIR

In the studied geothermal field, one doublet (P1 & I1) has already been drilled. Unfortunately, not much information and measurements are available, only a few logs are available from P1. Both wells are fully perforated at reservoir layers, from the top of Berkel Sandstone until the bottom of DelftSandstone. The first geothermal doublet is not in operation yet. The plan is that in a years' time another doublet (P2 and I2) will be added to this field. The arrangement of the wells, the operational schemes, and the static model have been provided by the asset owner. An intensive geological study has been conducted by a consultancy office based on surrounding boreholes and available logs, forming the static model used as bases case in this paper.

4.1 Reservoir Simulation

The mentioned geothermal reservoir is situated at a depth ranging between 1117 to 1965 meter. It has an average initial pressure of 200 bar and an average initial temperature of 348.15 K. Thermal and hydraulic properties of this field are presented in Table 1. In this model, doublet 1 is using a flow rate of 104 m^3/h and doublet 2 a rate of 416 m^3/h. Since no specific studies have been conducted on the sealing capability of the faults in this region, and furthermore both doublets are located far enough from the main faults, all faults are assumed to be open in this area.

For the numerical simulation of this geothermal system (unlike hydrocarbon simulations) all cells including sands and shales have been modeled (as active cells) for both heat and fluid transport to be able to capture the full effect of thermal convection in sands and thermal conduction in both sands and shales. In total, the dynamic model includes over 3,100,000 active cells. Figure 7 (top left) demonstrates a top view of the cold front propagation in the reservoir after 100 years of simulation.

Table 1: thermal and hydraulic properties of geothermal reservoir

Parameters Value	Unit	Value
Porosity	-	10^{-5} - 0.256
Permeability	mD	0.004-1308
Shale heat capacity	kJ/(m^3.K)	2300
Sand heat capacity	kJ/(m^3.K)	2450
Shale thermal conductivity	kJ/(m.day.K)	190
Sand thermal conductivity	kJ/(m.day.K)	260
Rate (P1 & I1)	m^3/h	104
Rate (P2 & I2)	m^3/h	416

4.2 Uncertainty Analysis

In this study, the provided static model by the asset owner has been taken as the base case (Figure 3). 100 realizations have been generated based on variation of the seed parameter in the base case facies model. The mean and standard deviation of parameters was kept as delivered and only spatial distribution (conditioned to up-scaled logs) has been varied. Initially, the facies have been generated using sequential indicator simulation for the Berkel Sandstone and object modeling for the channelized Delft Sandstone. Porosities have been generated by using Sequential Gaussian Simulation and permeabilities have been generated as co-kriging of porosity. Figure 4 shows some porosity realizations for the Berkel Sandstone and the Delft Sandstone.

By the asset owner, doublet one was positioned based on the undertaken uncertainty analysis. Doublet 2 was designed based on the updated model of the P50 case of the first doublet. It should be noted that the focus of both doublets is mainly placed on the Berkel Sandstone.

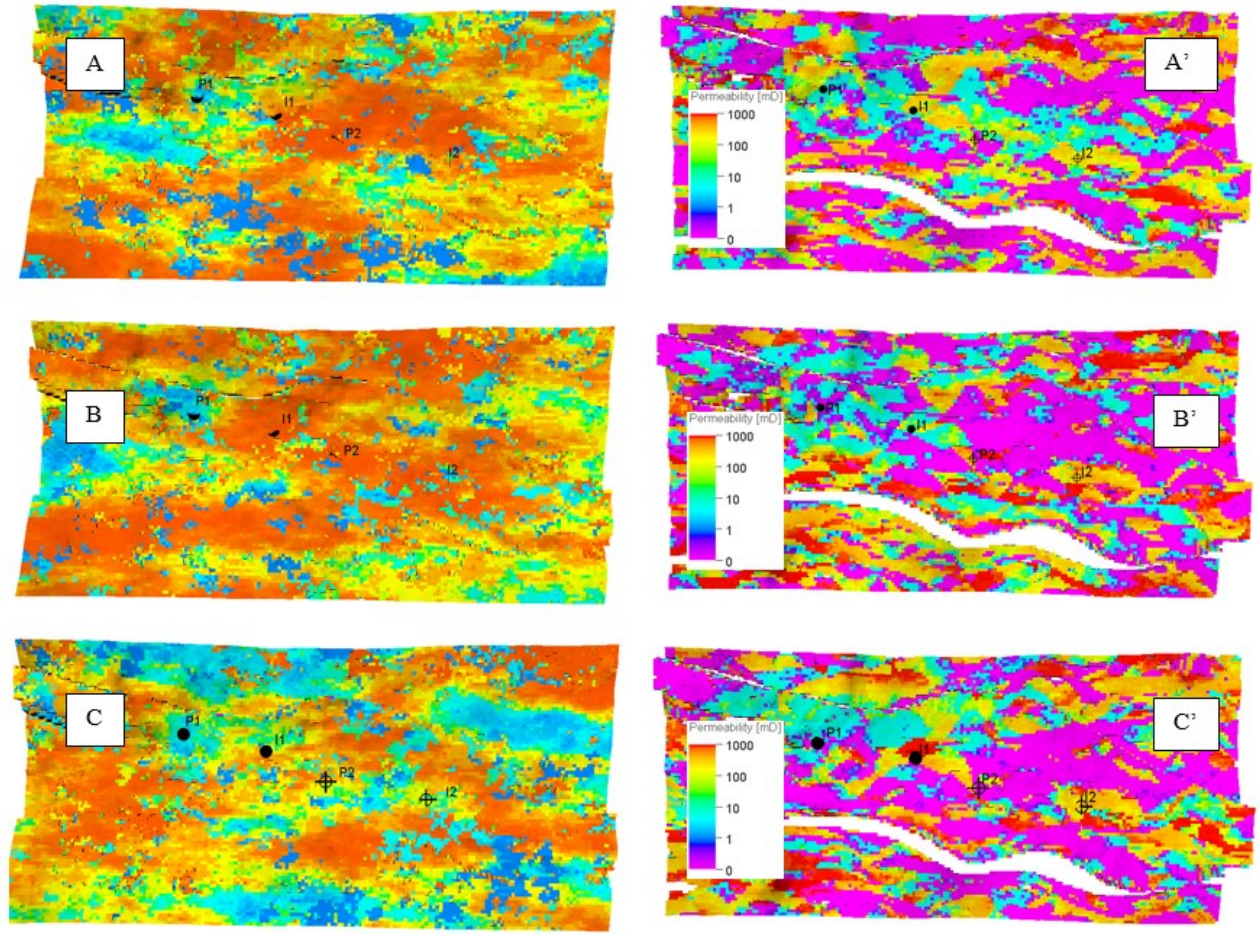

Figure 4: permeability in 3 different realizations. Left column: shows top of Berkel Sandstone, and right column: shows top of the Delft Sandstone.

5. RESULTS AND DISCUSSION

All 100 realizations where simulated numerically in DARTS. The fast computational time advantage of DARTS enabled us to complete this number of large (over 3,100,000 active cells) numerical modeling in about three days (running 2 simulations at a time) on a cluster node equipped with two Intel(R) Xeon(R) CPU E5-2640 v4 processors with 10 physical cores each and 252Gb RAM. The average model runtime is about 80 minutes, provided with total simulation period of 100 years, and maximum timestep of 365 days.

The production temperature of all realizations for doublet 1 and 2, are plotted in Figure 5. Similarly, the produced energy of the system over the time has plotted on Figure 6. For doublet 1 high (best) and low (worst) case scenarios has been identified which are showing the range of possible uncertainties of lifetime (in Figure 5-left) or produced energy (in Figure 6-left). Base, high, and low cases of the first doublet are plotted on the uncertainty range of doublet to show that, optimizing the well location based on the information and analysis of one set of wells (in this case doublet 1) does not necessarily lead to optimized results for the second doublet. As it can be seen in Figure 5 and Figure 6, the low case (worst case scenario) for doublet 1 is relatively a good case for doublet 2. Uncertainty of the facies model, especially at Delft Sandstone, hugely impacts the prediction of the lifetime and produced energy of doublets, and consecutively the whole geothermal system

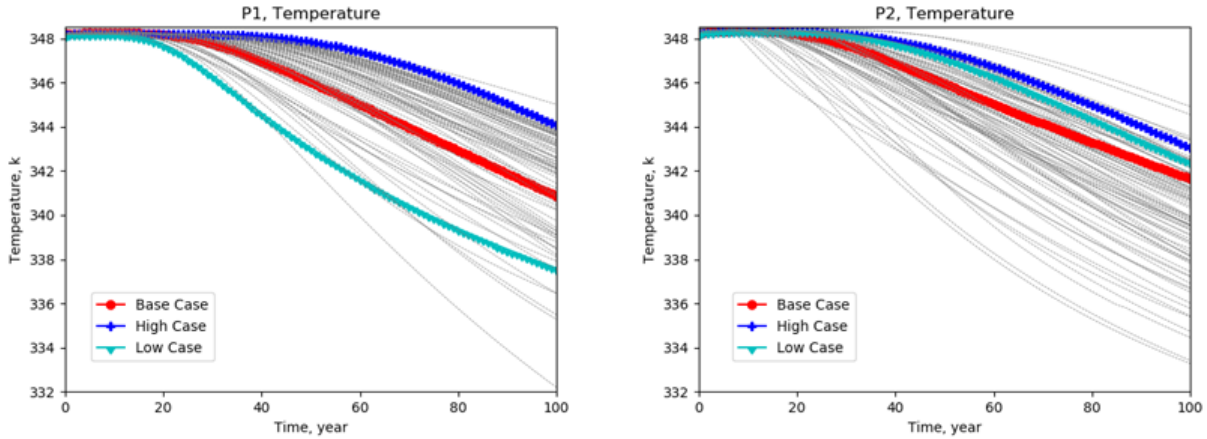

Figure 5: breakthrough curves of doublet 1 and 2.

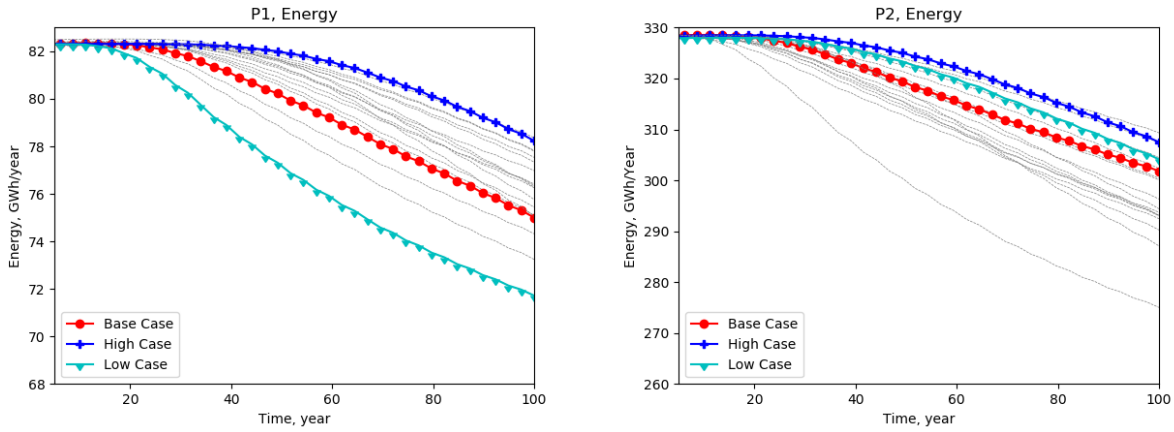

Figure 6: produced energy from doublet 1 and 2.

It can be clearly seen, from the results of doublet 2, how the lack of data in a geothermal field induces and increases uncertainty in the predictions of the lifetime and energy of the system. Considering lifetime as a time when initial production temperature drops by 2 degree Kelvin, the lifetime of doublet 1 (base case) is about 44 years, while the possible range (all cases) is between 33 and 79. For doublet 2, the lifetime (base case) is about 42 years, while the possible range (all cases) is between 20 and 84 years. This demonstrates the large uncertainty range of prediction in highly heterogeneous and channelized reservoirs.

If we project the uncertainty of life time (e.g., on the base case scenario) to the produced energy, the variation will be between 76 to 81.7 GWh for doublet 1 and between 310 to 330 GWh for doublet 2 (Figure 6). Looking to the wide ranges in lifetime and Energy of the system, the eventual NPV generation of such system can show even higher degrees of uncertainty. For such a heterogeneous reservoir, the value of any additional information about the subsurface that would help further constrain the model cannot be neglected. As previously shown, the geological uncertainty can have a significant impact to the system NPV (Daniilidis et al., 2017)

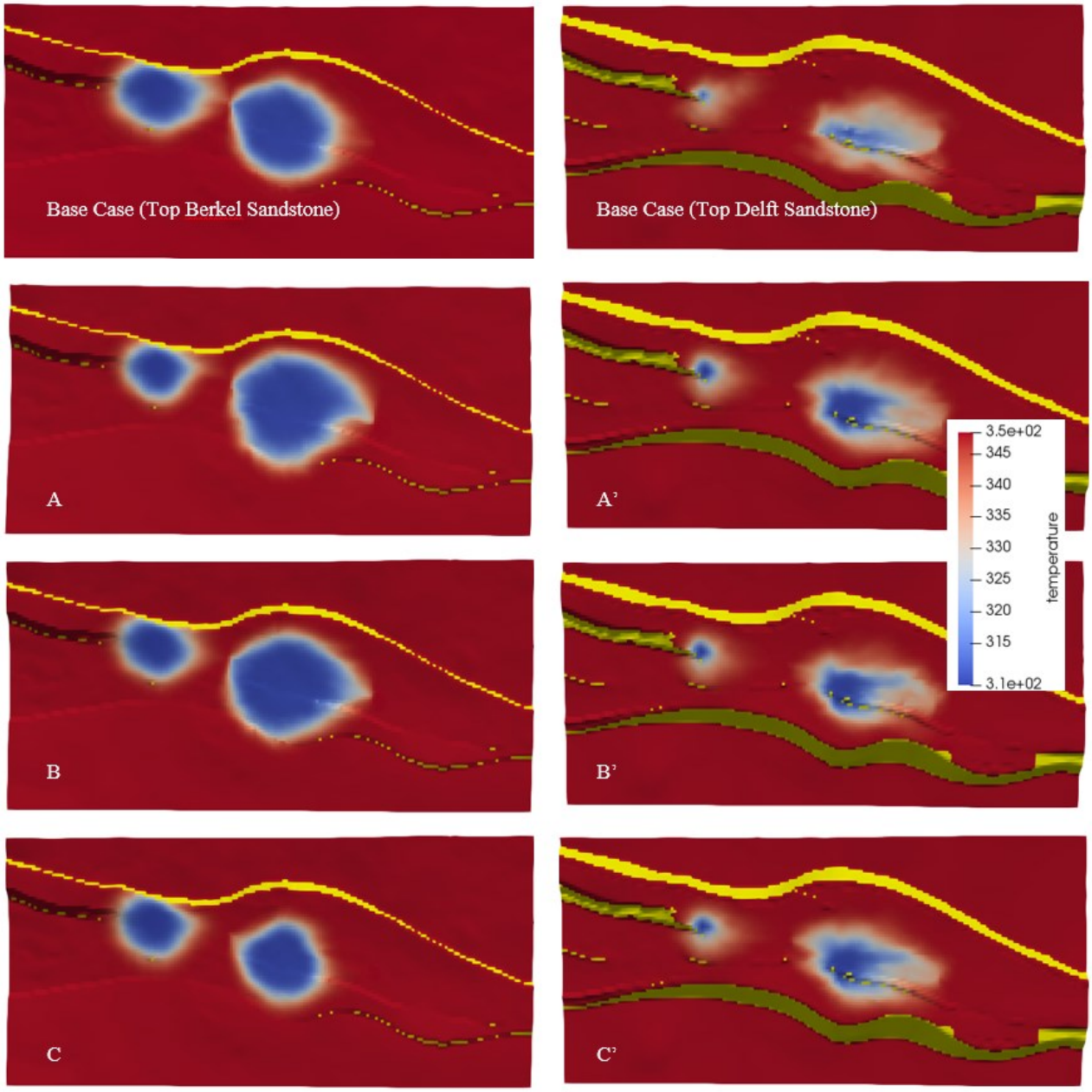

Figure 7: Cold front propagation in different scenarios. Left column shows the top of Berkel Sandstone and right column shows top of Delft Sandstone.

Figure 7 demonstrates the cold front propagation in the base case and 3 other scenarios after 100 years, in both Berkel and Delft Sandstones. Comparing Figure 4 and Figure 7 demonstrate that how variation in permeability (which is a result of variation in facies model) in different realizations, makes the cold front propagation and hence the lifetime very different. For instance looking to realization C in both figure, it is seen that Berekl Sandstone shows very poor reservoir characteristics hence its cold plume is very small compared to other realizations.

Looking to Figure 7, it can be clearly seen that the major part of heat is produced from Berkel reservoir. The variation in cold front propagation shape becomes more important if faults are present in the vicinity of the wells. In such case pressure distribution also become significant.

6.CONCLUSION

This paper tries to emphasize on the importance of exploration data in geothermal field development (studies) and decision making procedure by demonstrating how the uncertainty in facies model affects the predictions of geothermal field lifetime and produced energy.

In this paper, a real case study from south-west of the Netherlands has been studied. This reservoir consists of two main reservoir layers: one is an uniform sandstone; another consists of highly heterogeneous channelized sand bodies. Initially, uncertainty analysis is conducted based on few available log data in the vicinity of the first doublet. The base case study has been taken as a reference to design and model the second doublet. This study demonstrates how the lack of data can lead to misinterpretation of lifetime and produced energy of a geothermal system. In particular, the first doublet low case (worst case) scenario proves to be (in this study) a relatively good case scenario of doublet 2.

As a conclusion, in the presence of highly heterogeneous reservoirs more exploration data can facilitate having a better prediction of the system's lifetime and energy production, hence leading to a better field development procedure and enhanced decision making.

For further work, a suggestion to decrease the involved risk (while having no additional data) would be to focus individually on the production of each reservoir layers in both doublets. As Berkel Sandstone is not channelized hence less heterogeneous, it is expected to involve less uncertainty. Therefore, it might be better to optimize production mainly on Berkel reservoir.

7. REFERENCES

CBS: StatLine - Energiebalans; Aanbod, Omzetting En Verbruik." CBS: 1(2018). https://opendata.cbs.nl/statline/#/CBS/nl/dataset/83140NED/table?ts=1523353931286

Daniilidis, A., Alpsoy, B., Herber, R.: Impact of technical and economic uncertainties on the economic performance of a deep geothermal heat system. *Renew Energy*, **114**, (2017),805–816.

Daniilidis, A., Doddema, L., Herber, R.: Risk assessment of the Groningen geothermal potential: From seismic to reservoir uncertainty using a discrete parameter analysis. *Geothermics,* **64**, (201), 271–288.

DARTS: Delft Advanced Research Terra Simulator (2019). https://darts.citg.tudelft.nl.

Donselaar, M.E., Groenenberg, R.M., Gilding, D.T., Address, M.: Reservoir Geology and Geothermal Potential of the Delft Sandstone Member in the West Netherlands Basin, *Proceedings World Geothermal Congress*, (2015).

Faust, C. R. and Mercer, J. W.: Summary of Our Research in Geothermal Reservoir Simulation. Proceedings. In *Workshop on Geothermal Reservoir Engineering*, Stanford University, Stanford, (1975).

Fernández, M., Eguía, P., Granada, E., Febrero, L.: Sensitivity Analysis of a Vertical Geothermal Heat Exchanger Dynamic Simulation: Calibration and Error Determination. *Geothermics,* **70**, (2017): 249–59.

"Geothermal Well." https://www.tudelft.nl/geothermalwell/

Khait, M. and Voskov, D.: GPU-offloaded general-purpose simulator for multiphase flow in porous media. *SPE Reservoir Simulation Conference*, (2017).

Khait, M. and Voskov, D.: Operator-based linearization for efficient modeling of geothermal processes, *Geothermics*, **74**, (2018), 7-18.

Khait, M., Voskov, D. : "Integrated framework for modelling of thermal-compositional multiphase flow in porous media", *SPE Reservoir Simulation Conference*, (2019).

PanTerra Geoconsultants, "Project report: G1330c", March 2018.

Saeid, S., Al-Khoury, R., Nick, H. M., Hicks, M. A.: A prototype design model for deep low-enthalpy hydrothermal systems. *Renewable energy*, **77**, (2015), 408-422.

Vogt, C., Mottaghy, D., Rath, V., Wolf, A., Pechnig, R., & Clauser, C.: Quantifying Uncertainties in Geothermal Energy Exploration Quantifying Uncertainty in Geothermal Reservoir Modeling. Proceedings World Geothermal Congress, (2010).

Voskov, D.: Operator-based linearization approach for modeling of multiphase multi-component flow in porous media, *Journal of Computational Physics*, **337**,(2017), 275-288.

Watanabe, N., Wang, W., McDermott, C. I., Taniguchi, T., & Kolditz, O. : Uncertainty analysis of thermo-hydro-mechanical coupled processes in heterogeneous porous media, *Computational Mechanics*, **45(4),** (201), 263.

Wang, Y., Khait, M., Voskov, D., Saeid, S. and Bruhn, D.: Benchmark test and sensitivity analysis for Geothermal Applications in the Netherlands. *44th Workshop on Geothermal Reservoir Engineering*, Stanford (2019).

Willems, C.J.L., and H. M. Nick. "Towards Optimisation of Geothermal Heat Recovery: An Example from the West Netherlands Basin." *Applied Energy, **247**(2019) 582–93*.

Wong, Z.Y., Horne, R., Voskov, D.: A Geothermal Reservoir Simulator in AD-GPRS, *Proceedings World Geothermal Congress*, (*2015)*.